Wide viewing angle dynamic holographic stereogram with a curved array of spatial light modulators

Joonku Hahn, Hwi Kim, Yongjun Lim, Gilbae Park, and Byoungho Lee

School of Electrical Engineering, Seoul National University, Gwanak-Gu Sillim-Dong, Seoul 151-744, Korea
byoungho@snu.ac.kr
http://oeqelab.snu.ac.kr

Abstract: A novel design of dynamic holographic stereogram with a curved array of spatial light modulators (SLMs) is proposed. In general, it is difficult to simultaneously achieve a wide viewing angle and an available width for the digital holographic display. Moreover, the wide viewing angle of a display system needs a large optical numerical aperture where the paraxial approximation fails, and thus an extremely large planar SLM is necessary in using previous methods. To solve this problem, our proposed display system is composed of a curved array of SLMs to obtain a large number of data points and reduce the spatial bandwidth in SLMs. In the curved array of SLMs, each SLM is individually transformed to display local angular spectra of object wave, which is based on a fundamental idea of holographic stereogram. To embody the dynamic holographic stereogram with SLMs, each SLM is effectively reformed for simplifying the optical structure and reducing the light power loss. In detail, spatially modulated wave is optically divided and transformed, as if each SLM were composed of three sub-SLMs. This design improves the scalability in viewing angle of holographic display and the loss of light power is significantly reduced. With this method, we can achieve the digital holographic display with 22.8° viewing angle.

OCIS codes: (070.2580) Paraxial wave optics; (090.1760) Computer holography; (230.6120) Spatial light modulators.

References and links

1. P. Benzie, J. Watson, P. Surman, I. Rakkolainen, K. Hopf, H. Urey, V. Sainov, and C. von Kopylow, “A survey of 3DTV displays: techniques and technologies,” IEEE Trans. Circuits Syst. Video Technol. **17**, 1647-1658 (2007).
2. M. Kovachev, R. Ilieva, P. Benzie, G. B. Esmer, L. Onural, J. Watson, and T. Reyhan, “Holographic displays using spatial light modulators,” in *Three-Dimensional Television: Capture, Transmission, and Display*, H. M. Ozaktas and L. Onural, eds., (Springer Verlag, 2007), pp. 529-556.
3. L. Onural, A. Gotchev, H. M. Ozaktas, and E. Stoykova, “A survey of signal processing problems and tools in holographic three-dimensional television,” IEEE Trans. Circuits Syst. Video Technol. **17**, 1631-1646 (2007).
4. N. Fukaya, K. Maeno, O. Nishikawa, K. Matumoto, K. Sato, and T. Honda, “Expansion of the image size and viewing zone in holographic display using liquid crystal devices,” Proc. SPIE **2406**, 283-289 (1995).
5. K. Maeno, N. Fukaya, O. Nishikawa, K. Sato, and T. Honda, “Electro-holographic display using 15 mega pixels LCD,” Proc. SPIE **2652**, 15-23 (1996).
6. C. Slinger, P. Brett, V. Hui, G. Monnington, D. Pain, and I. Sage, “Electrically controllable multiple, active, computer-generated hologram,” Opt. Lett. **22**, 1113-1115 (1997).
7. M. Stanley, R. W. Bannister, C. D. Cameron, S. D. Coomber, I. G. Cresswell, J. R. Hughes, V. Hui, P. O. Jackson, K. A. Milham, R. J. Miller, D. A. Payne, J. Quarrel, D. C. Scattergood, A. P. Smith, M. A. Smith, D. L. Tipton, P. J. Watson, P. J. Webber, and C. W. Slinger, “100 mega-pixel computer generated holographic images from active tiling--a dynamic and scalable electro-optic modulator system,” Proc. SPIE **5005**, 247-258 (2003).

#96374 - $15.00 USD Received 19 May 2008; revised 26 Jul 2008; accepted 30 Jul 2008; published 1 Aug 2008

8. C. W. Slinger, C. D. Cameron, S. D. Coomber, R. J. Miller, D. A. Payne, A. P. Smith, M. G. Smith, M. Stanley, and P. J. Watson, "Recent developments in computer-generated holography: toward a practical electroholography system for interactive 3D visualization," Proc. SPIE **5290**, 27-41 (2004).
9. J. T. McCrickerd and N. George, "Holographic stereogram from sequential component photographs," Appl. Phys. Lett. **12**, 10-12 (1968).
10. S. A. Benton, "Survey of holographic stereograms," Proc. SPIE **367**, 15-19 (1983).
11. J. R. Andrews, J. E. Stinehour, M. H. Lean, D. O. Potyondy, P. A. Wawrzynek, A. R. Ingraffea, and M. D. Rainsdon, "Holographic display of computer simulations," Proc. SPIE **1461**, 110-123 (1991).
12. M. W. Halle, S. A. Benton, M. A. Klug, and J. S. Underkoffler, "The ultragram: a generalized holographic stereogram," Proc. SPIE **1461**, 142-155 (1991).
13. T. Yatagai and Y. Sando, "Phase-shifting digital holography," in *Digital Holography and Three-dimensional Display*, T.-C. Poon, ed., (Springer, 2006), pp. 257-272.
14. M. Yamaguchi, H. Endoh, T. Honda, and N. Ohyama, "High-quality recording of a full-parallax holographic stereogram with a digital diffuser," Opt. Lett. **19**, 135-137 (1994).
15. S. Chen and M. R. Chatterjee, "Implementation of a spatially multiplexed pixelated three-dimensional display by use of a holographic optical element array," Appl. Opt. **37**, 7504-7513 (1998).
16. S. Shin and B. Javidi, "Speckle-reduced three-dimensional volume holographic display by use of integral imaging," Appl. Opt. **41**, 2644-2649 (2002).
17. S. Shin and B. Javidi, "Viewing-angle enhancement of speckle-reduced volume holographic three-dimensional display by use of integral imaging," Appl. Opt. **41**, 5562-5567 (2002).
18. K. Choi, J. Kim, Y. Lim, and B. Lee, "Full parallax viewing-angle enhanced computer-generated holographic 3D display system using integral lens array," Opt. Express **13**, 10494-10502 (2005).
19. J. W. Goodman, *Introduction to Fourier Optics*, 3rd ed. (Roberts & Company Publishers, 2004).
20. M. J. Bastiaans, "Transport equations for the Wigner distribution function," Opt. Acta **26**, 1265–1272 (1979).
21. Y. Kim, J.-H. Park, S.-W. Min, S. Jung, H. Choi, and B. Lee, "Wide-viewing-angle integral three-dimensional imaging system by curving a screen and a lens array," Appl. Opt. **44**, 546-552 (2005).
22. J. Hahn, H. Kim, and B. Lee, "Optimization of the spatial light modulation with twisted nematic liquid crystals by a genetic algorithm," Appl. Opt. **47**, D87-D95 (2008).
23. H. Kim, J. Hahn, and B. Lee, "Mathematical modeling of triangle mesh-modeled three-dimensional surface objects for digital holography," Appl. Opt. **47**, D117-D127 (2008).

1. Introduction

Holographic display is the most fundamental technology for displaying three-dimensional (3D) object since the object wavefront can be correctly reconstructed [1]. To modulate the coherent wave dynamically, various spatial light modulators (SLMs) have been applied to holographic display in many studies. Recently, on the account of the growth of display industry, liquid crystal SLMs are regarded as the most feasible devices for embodying holographic display [2, 3]. However, they have restricted numbers of data points, e.g., a few million pixels. The number of data points is closely related to the viewing volume which is represented as the width of display and viewing angle. In order to increase the data points of holographic display, the technology of tiling plural SLMs is necessary.

The technology of tiling several SLMs using a large beam splitter were proposed by Fukaya *et al* [4, 5]. In this method, SLMs are aligned at both side of the beam splitter at regular intervals and the combined modulated waves by the beam splitter are comparable to the case of using a large seamless SLM. Slinger *et al.* proposed another tiling method with sequential arrangement of electrically and optically addressed SLMs [6-8]. In these systems, a high-speed driven electrically addressed SLM is able to control 25 optically addressed SLMs, which constitute a single channel. And then several channels can be aligned to form a flat hologram with large data points. However, these technologies apply a single Fourier transforming optics to cover the whole SLMs and thus it is difficult to achieve a wide viewing angle display, since it needs a large numerical aperture of optics where the paraxial approximation fails and an extremely large SLM is necessary.

The main idea to solve these problems can be found in the holographic stereogram. Holographic stereogram is a remarkable technology which can reduce the bandwidth of hologram by defining viewing scope by a viewing window [9-13]. In general, a viewing slit is used as the viewing window for holographic stereogram and 3D views are recorded in holographic materials by a coherent light source. By extending one-dimensional (1D) viewing slit to two-dimensional (2D) square aperture, full-parallax holographic recording is possible

#96374 - $15.00 USD Received 19 May 2008; revised 26 Jul 2008; accepted 30 Jul 2008; published 1 Aug 2008

[14]. These early studies use optical stops for defining viewing scope. As an alternative method, some full-parallax holographic stereograms are realized with the help of holographic optical elements [15] or lens array [16, 17]. These techniques use a 2D array of optics which does not refract chief rays from entrance pupil to exit pupil. They are beneficial to the simultaneous record of every viewing scopes defined by correspondent constituent optics. The bandwidth of hologram is limited by the interval between these constituents.

To overcome static properties of holographic materials, various holographic stereograms using an SLM have been studied and the digital holographic stereogram with a lens array and a single SLM were proposed [18]. However, this system does not have sufficient data points and the planar SLM is not suitable for wide viewing angle.

In this paper, we propose a dynamic holographic stereogram with a curved array of SLMs to obtain a large number of data points and reduce the spatial bandwidth in SLMs. In the curved array of SLMs, each SLM is individually transformed to display local angular spectra of object wave. Moreover, we reform SLM shape effectively to simplify the optical structure and reduce the light power loss. Each SLM has individual transfer optics with folding mirrors and spatially modulated wave is optically divided and transformed, as if each SLM were composed of three sub-SLMs. Here, these sub-SLMs are regarded as positioned diagonally and the viewing fields of them are extended continuously without interruption. This design improves the scalability in viewing angle of holographic stereogram and the loss of light power is significantly reduced with no use of beam splitters.

This paper is organized as follows. In Sec. 2, the general constraint in field of view by a single SLM is expressed analytically. In Sec. 3, the field of view by the proposed curved array of SLMs is explained. In Sec. 4, the structure of the effectively reformed SLM is described and the benefit of this design is detailed. In Sec. 5, the embodiment of dynamic holographic stereogram with proposed techniques is explained. In Sec. 6, experimental results are presented and discussed. In Sec. 7, conclusion and perspective are given.

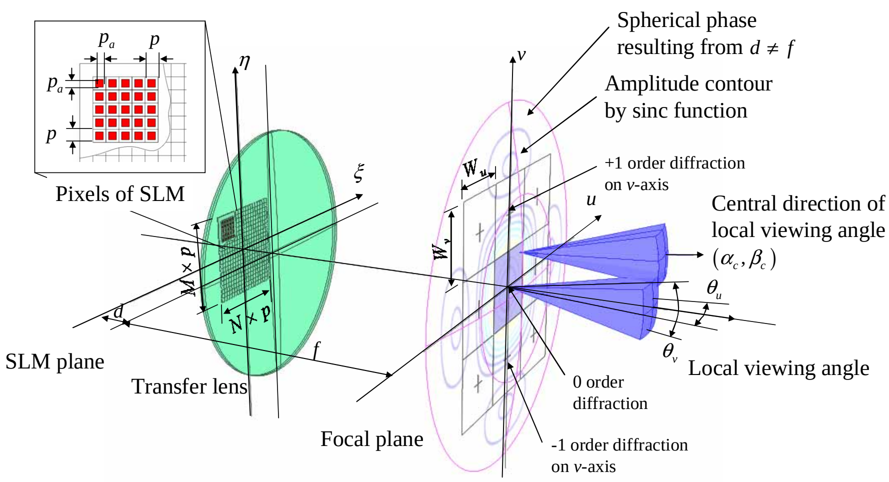

Fig. 1. Local viewing angles in field of view displayed by a single SLM.

2. Field of view generated by a single SLM

In this section, the field of view displayed by a single SLM is formulated within paraxial approximation. Local angular spectrum is defined using the Wigner distribution function and the relation between area and local viewing angles in reconstructed field of view is presented. The total viewing angle of holographic display with an SLM is calculated with the help of transportation of Wigner distribution function. The significance of data points in holographic display is discussed.

#96374 - $15.00 USD Received 19 May 2008; revised 26 Jul 2008; accepted 30 Jul 2008; published 1 Aug 2008

Figure 1 shows the field of view at focal plane displayed by a single SLM. The SLM is transferred by a lens and generates the reconstructed field, which is defined by the product of transverse area and viewing angle at focal plane. From Ref. 19, the reconstructed wave at the focal plane is determined by

$$U_f(u,v)=\frac{A}{j\lambda f}\exp\left[j\frac{k}{2f}\left(1-\frac{d}{f}\right)\left(u^2+v^2\right)\right]\iint U_i(\xi,\eta)P\left(\xi+\frac{d}{f}u,\eta+\frac{d}{f}v\right)\exp\left[-j\frac{2\pi}{\lambda f}(\xi u+\eta v)\right]d\xi d\eta. \tag{1}$$

Here, d is the distance between SLM and transfer lens with focal length f. The modulated wave by SLM with $(N+1)\times(M+1)$ data points at SLM plane is given by

$$U_i(\xi,\eta)=\sum_{n=0}^{n=N}\sum_{m=0}^{m=M}U_i(n,m)\delta\left[\xi-(n-N/2)p\right]\delta\left[\eta-(m-M/2)p\right]\otimes rect(\xi/p_a)rect(\eta/p_a). \tag{2}$$

Here, p and p_a are pixel pitch and pixel aperture of SLM, respectively. And $U_i(n,m)$ means the value of modulation by the pixel located at point (n,m). If the pupil of lens is large enough in comparison with the diffraction field by pixel aperture p_a, the wave at the focal plane is briefly expressed as

$$\begin{aligned}U_f(u,v)=&\frac{A{p_a}^2}{j(\lambda f)^3}\exp\left[j\frac{k}{2f}\left(1-\frac{d}{f}\right)\left(u^2+v^2\right)\right]\times\mathrm{sinc}\left(\frac{p_a u}{\lambda f}\right)\mathrm{sinc}\left(\frac{p_a v}{\lambda f}\right)\\&\times\sum_{n=0}^{n=N}\sum_{m=0}^{m=M}U_i(n,m)\exp\left\{-\frac{j2\pi p}{\lambda f}\left[(n-N/2)u+(m-M/2)v\right]\right\}.\end{aligned} \tag{3}$$

Here, the first exponential term is the spherical phase resulting from inequality of distance d and focal length f. The second term (sinc function) is determined by the pixel aperture p_a. It is not complex value and has influence on the amplitude of reconstructed field. And the last summation term is understood as Fourier series expansion. Therefore, the width of display, i.e., the transverse period of wave is given by

$$W_u=\lambda f/p, \tag{4a}$$

$$W_v=\lambda f/p. \tag{4b}$$

Generally, angular spectrum is defined as the integral over the whole plane. To analyze the field of view at the fixed position, the definition of local angular spectrum is needed. By the use of Wigner distribution function, the local angular spectrum at position (u,v) can be represented as

$$W\left(u,v,\frac{\alpha}{\lambda},\frac{\beta}{\lambda};0\right)=\iint U_f(u+u'/2,v+v'/2){U_f}^*(u-u'/2,v-v'/2)\exp\left[-j2\pi\left(\frac{\alpha}{\lambda}u'+\frac{\beta}{\lambda}v'\right)\right]du'dv'. \tag{5}$$

Here, (α,β) means the directional cosines and the zero means the propagation length along the *z*-axis from focal plane. By the projection property, the Wigner distribution function is related with the angular spectrum as

$$\left|A\left(\frac{\alpha}{\lambda},\frac{\beta}{\lambda};0\right)\right|^2=\iint W\left(u,v,\frac{\alpha}{\lambda},\frac{\beta}{\lambda};0\right)dudv. \tag{6}$$

Here, the definition of local angular spectrum by Wigner distribution function has universal validity. By Eq. (3), the local angular spectrum of reconstructed field at position (u,v) is given by

#96374 - $15.00 USD Received 19 May 2008; revised 26 Jul 2008; accepted 30 Jul 2008; published 1 Aug 2008

$$W\left(u,v,\frac{\alpha}{\lambda},\frac{\beta}{\lambda};0\right)=\frac{16|A|^2}{(\lambda f)^2}\sum_{n_1=0}^{n_1=N}\sum_{m_1=0}^{m_1=M}\sum_{n_2=0}^{n_2=N}\sum_{m_2=0}^{m_2=M}U_i(n_1,m_1)U_i^*(n_2,m_2)\exp\left\{-\frac{j2\pi p}{\lambda f}\left[(n_1-n_2)u+(m_1-m_2)v\right]\right\}$$
$$\times\Lambda\left\{\frac{2\lambda f}{p_a}\left[\frac{\alpha}{\lambda}-\frac{1}{\lambda f}\left(1-\frac{d}{f}\right)u-\frac{p(n_1+n_2-N)}{2\lambda f}\right]\right\}\Lambda\left\{\frac{2\lambda f}{p_a}\left[\frac{\beta}{\lambda}-\frac{1}{\lambda f}\left(1-\frac{d}{f}\right)v-\frac{p(m_1+m_2-M)}{2\lambda f}\right]\right\}. \quad (7)$$

Here, the span of triangle function results from the sinc function with the pixel aperture p_a. If the effect of the span of triangle function is neglected, the local angular spectrum could be represented as delta functions of directional cosines (α,β). Therefore, the central direction of viewing angle at position (u,v) is given by

$$(\alpha_c,\beta_c)=\frac{1}{f}\left(1-\frac{d}{f}\right)(u,v). \quad (8)$$

And by paraxial approximation, the local viewing angles are given by

$$\theta_u \approx \Delta\alpha = Np/f, \quad (9a)$$

$$\theta_v \approx \Delta\beta = Mp/f. \quad (9b)$$

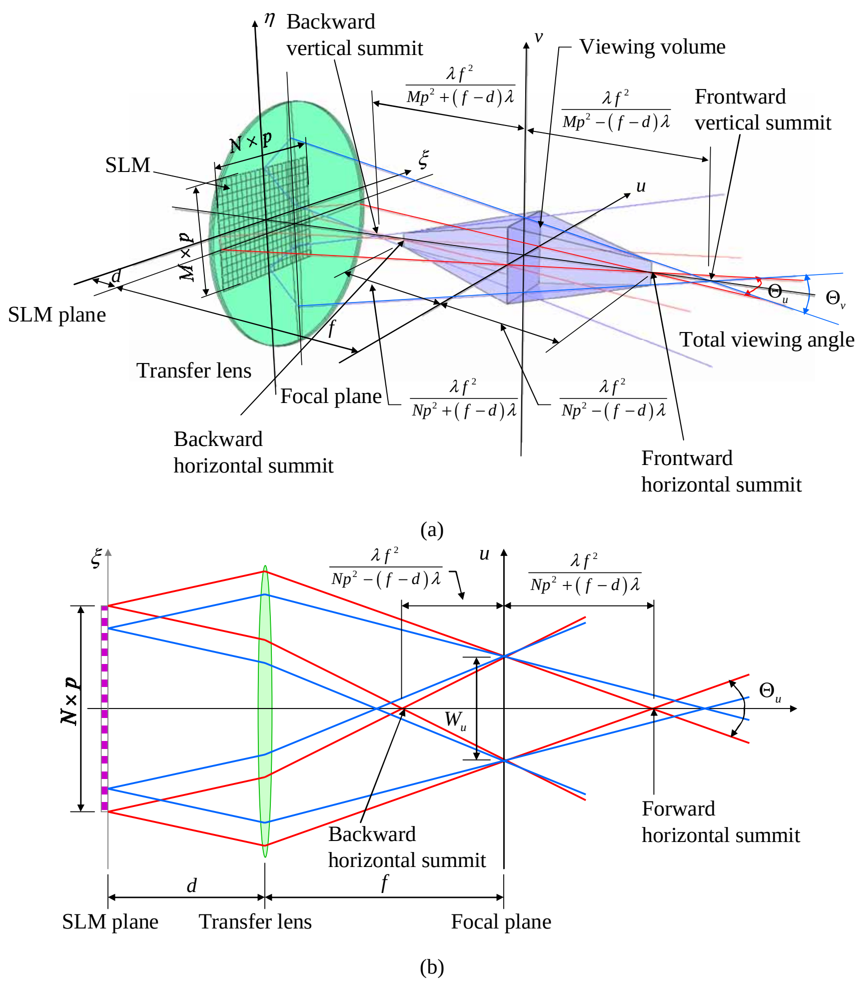

Fig. 2. Total viewing angles in field of view displayed by a single SLM in (a) three dimensional view and (b) planar view.

#96374 - $15.00 USD Received 19 May 2008; revised 26 Jul 2008; accepted 30 Jul 2008; published 1 Aug 2008

Therefore, two significant parameters, the area and local viewing angles of reconstructed field at focal plane satisfy the following relation

$$W_u W_v \theta_u \theta_v / \lambda^2 \approx N \times M. \tag{10}$$

In Eq. (10), the product of area and local viewing angles at a wavelength is equal to the number of data points of SLM. This equation has a significant meaning that the product of widths and local viewing angles is independent of the optical parameters of transfer optics and determined by the number of pixels in SLM. Therefore, for a fixed number of data points, it is impossible to enhance the local viewing angle without the cost of view width in a digital holographic display.

As previously mentioned, the reconstructed field at focal plane is expanded as Fourier series, and the effective region to display within Nyquist frequencies is restricted within the transverse periods of wave at focal plane as follows:

$$W_N\left(u,v,\frac{\alpha}{\lambda},\frac{\beta}{\lambda};0\right)=W\left(u,v,\frac{\alpha}{\lambda},\frac{\beta}{\lambda};0\right)rect\left(\frac{pu}{\lambda f}\right)rect\left(\frac{pv}{\lambda f}\right). \tag{11}$$

The transport equation can be formulated in geometrical optical terms in a homogeneous medium and the Wigner distribution function has a constant value along a geometrical optical light ray from Ref. 20. That is, along the optical path $\vec{s}$ in free space, the Wigner distribution remains constant which is represented as

$$dW\left(u,v,\frac{\alpha}{\lambda},\frac{\beta}{\lambda};0\right)\Big/ d\vec{s}=0. \tag{12}$$

Therefore, the transportation of Wigner distribution function is given by

$$W\left(u,v,\frac{\alpha}{\lambda},\frac{\beta}{\lambda};z\right)=W\left(u-\frac{\alpha}{\gamma}z,v-\frac{\beta}{\gamma}z,\frac{\alpha}{\lambda},\frac{\beta}{\lambda};0\right). \tag{13}$$

Here, directional cosine γ is defined by

$$\gamma=\sqrt{1-\alpha^2-\beta^2}. \tag{14}$$

Form Eqs. (7), (11), and (13), the Wigner distribution function at a distance z from the focal plane is represented as

$$\begin{aligned}
W_N\left(u,v,\frac{\alpha}{\lambda},\frac{\beta}{\lambda};z\right)=&\frac{16|A|^2}{(\lambda f)^2}\sum_{n_1=0}^{n_1=N}\sum_{m_1=0}^{m_1=M}\sum_{n_2=0}^{n_2=N}\sum_{m_2=0}^{m_2=M}U_i(n_1,m_1)U_i^*(n_2,m_2)\\
&\times\exp\left\{-\frac{j2\pi p}{\lambda f}\left[(n_1-n_2)\left(u-\frac{\alpha}{\gamma}z\right)+(m_1-m_2)\left(v-\frac{\beta}{\gamma}z\right)\right]\right\}\\
&\times\Lambda\left\{\frac{2\lambda f}{p_a}\left[\frac{\alpha}{\lambda}-\frac{1}{\lambda f}\left(1-\frac{d}{f}\right)\left(u-\frac{\alpha}{\gamma}z\right)-\frac{p(n_1+n_2-N)}{2\lambda f}\right]\right\}\\
&\times\Lambda\left\{\frac{2\lambda f}{p_a}\left[\frac{\beta}{\lambda}-\frac{1}{\lambda f}\left(1-\frac{d}{f}\right)\left(v-\frac{\beta}{\gamma}z\right)-\frac{p(m_1+m_2-M)}{2\lambda f}\right]\right\}\\
&\times rect\left[\frac{p}{\lambda f}\left(u-\frac{\alpha}{\gamma}z\right)\right]rect\left[\frac{p}{\lambda f}\left(v-\frac{\beta}{\gamma}z\right)\right].
\end{aligned} \tag{15}$$

Equation (15) defines the field of view displayed by an SLM as shown in Fig. 2. In Fig. 2(a), this wedge-shaped viewing volume has four summits if the horizontal and vertical pixel numbers satisfy the following conditions:

 Received 19 May 2008; revised 26 Jul 2008; accepted 30 Jul 2008; published 1 Aug 2008

$$N < (f-d)\lambda/p^2, \tag{16a}$$

$$M < (f-d)\lambda/p^2. \tag{16b}$$

Figure 2(b) shows a planar view of this wedge-shaped viewing volume. With a fixed pixel aperture p_a of SLM, the distance between the backward and forward summits increases according as the data points of SLM decreases. That is, the viewing volume generated by a small data points is bigger than that by a large data points. This relation is reasonable since the viewing volume is defined as the reconstructed field of view within the Nyquist frequency by SLM. Therefore the viewing volume by a small data points is represented as the relatively small number of frequencies.

In these summits, front summits define the total viewing angles and in paraxial approximation, these angles are given by

$$\Theta_u \approx 2\tan^{-1}\left[\frac{Np}{2f} - \frac{\lambda}{2p}\left(1-\frac{d}{f}\right)\right] = 2\tan^{-1}\left[\frac{\lambda N}{2W_u} - \frac{\lambda}{2p}\left(1-\frac{d}{f}\right)\right], \tag{17a}$$

$$\Theta_v \approx 2\tan^{-1}\left[\frac{Mp}{2f} - \frac{\lambda}{2p}\left(1-\frac{d}{f}\right)\right] = 2\tan^{-1}\left[\frac{\lambda M}{2W_v} - \frac{\lambda}{2p}\left(1-\frac{d}{f}\right)\right]. \tag{17b}$$

From Eqs (17a) and (17b), for the fixed distance d, the total viewing angle is represented in proportion to the data points in the SLM and in inverse proportion to the width of reconstructed field at focal plane. Therefore, in order to display 3D objects having wide viewing angle with available width, the technology increasing the data points of SLM is necessary. The technique of tiling plural SLMs is a practical solution to overcome this restriction in the data points of a single SLM.

3. Field of view generated by a curved array of SLMs

In this section, relationship between angular spectrum and spatial frequencies of object wave is discussed and their recording positions on the holograms are described. The problems are explained to display a wide viewing angle with a planar array of SLMs. The field of view displayed by a curved array of SLMs is described and the total viewing angle in a curved array of SLMs is formulated.

Figure 3 shows a conventional planar hologram and a curved holographic stereogram. In Fig. 3(a), the angular spectrum of object wave is totally transferred by lens and in Fig. 3(b), the angular spectrum is locally transferred by lenses with viewing windows. In the object wave, angular spectrum with the angle ϕ_U between the directional cosine and *z*-axis is represented as the spatial frequency f_U following the relation of

$$\phi_U = 2\tan^{-1}(\lambda f_U). \tag{18}$$

Here, λ means the wavelength of object wave. In a conventional planar hologram, the high spatial frequencies are recorded on the portion of hologram which is located far from the optical axis. Therefore, the conventional planar hologram to display wide viewing angle violates the paraxial approximation. Moreover, in Eq. (18), the directional cosine of angular spectrum and its spatial frequency is related with tangent function and in order to increase angular spectrum displayed by a hologram, the width of the hologram should increase abruptly as the tangent function.

#96374 - $15.00 USD Received 19 May 2008; revised 26 Jul 2008; accepted 30 Jul 2008; published 1 Aug 2008

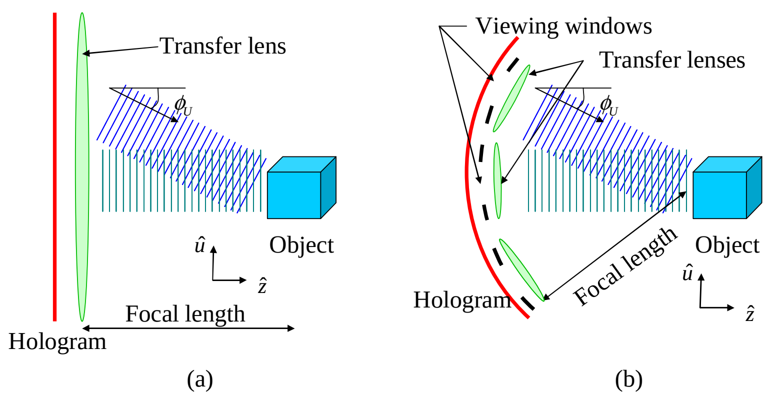

Fig. 3. Angular spectrum of object wave and their recording positions on (a) a conventional planar hologram and (b) a curved holographic stereogram.

In this paper, we solve these problems with techniques based on holographic stereogram. In the curved holographic stereogram, each portion of the hologram is locally transformed and its partial wave represents local angular spectrum with the small spatial bandwidth as shown in Fig. 3(b). The individual viewing window defines the range of angular spectrum and the corresponding lens transfers the object wave to the hologram. Although a structure using a curved screen with curved lens array was proposed for integral imaging [21], the curved structure for digital holography to present a huge data point set was not proposed before, to the authors' knowledge.

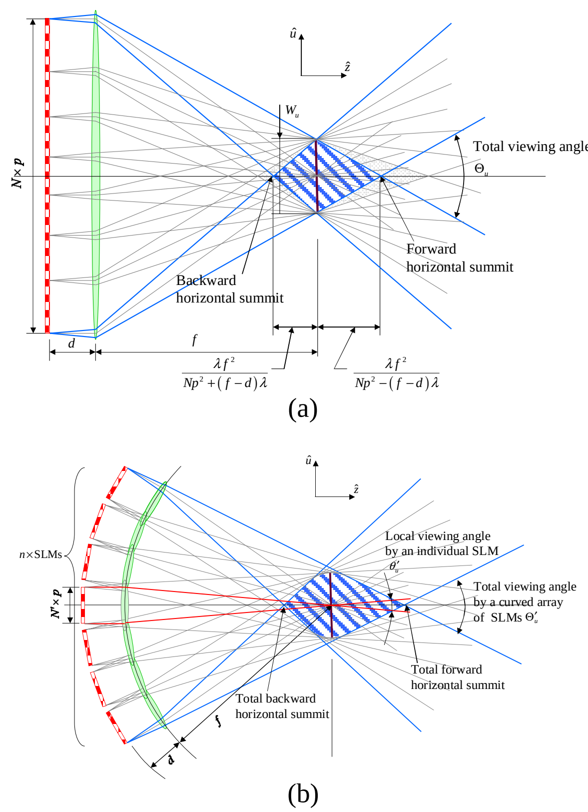

Fig. 4. Fields of view displayed by (a) a conventional planar SLM and (b) a curved array of SLMs.

#96374 - $15.00 USD Received 19 May 2008; revised 26 Jul 2008; accepted 30 Jul 2008; published 1 Aug 2008

The Field of view displayed by the proposed curved array of SLMs is represented as the composition of the field of views displayed by a single SLM. In this paper, we construct the dynamic holographic stereogram with horizontal parallax only (HPO) and the discussion on the field of view is limited within *uz*-plane. Figure 4 shows fields of view displayed by a conventional planar SLM and a curved array of SLMs. In Fig. 4(a), the summits of viewing volume exist when Eq. (16a) is satisfied and the total viewing angle is given by Eq. (17a). In Fig. 4(b), even if Eq. (16a) is not satisfied, the viewing volume can be defined. In field of view displayed by n units of SLMs with N' horizontal pixels, the total viewing angle is given by

$$\begin{aligned}\Theta'_u &= (n-1)\theta'_u + 2\tan^{-1}\left[\frac{N'p}{2f} - \frac{\lambda}{2p}\left(1-\frac{d}{f}\right)\right] \\ &= \frac{(n-1)N'p}{f} + 2\tan^{-1}\left[\frac{N'p}{2f} - \frac{\lambda}{2p}\left(1-\frac{d}{f}\right)\right].\end{aligned} \tag{19}$$

Here, θ' means the local viewing angle by an individual SLM and it is equal to the rotation angle between two adjacent SLMs. And f is the focal length of a local transfer lens and it is the same as the radius of curvature on which transfer lenses are aligned. From Eq. (19) the total viewing angle is the sum of the angle between two terminal SLMs and the local viewing angle by a unit SLM. For the limit case with large n and relatively small N', the total viewing angle is linearly proportional to the whole horizontal pixel number, nN'. Therefore, the proposed structure with a curved array of SLMs has an advantage to enhance the total viewing angle of holographic display in comparison with a conventional planar array of SLMs.

4. Effectively reformed SLM with scalability

In this section, the field of view displayed by effectively reformed SLM is described and the benefit of this design is discussed. The structure of the proposed effectively reformed SLM is detailed and viewing directions in array of these units are explained. And in upper arm of this unit, the quality deterioration resulting from folding optics is discussed.

The total viewing angle of holographic stereogram with a curved array of SLMs is closely related with the local viewing angle of a unit SLM and the number of them. In this paper, we present an HPO holographic stereogram with the help of asymmetric diffusing screen. Therefore, vertical viewing angles of SLMs are not distinguishable and there is a room to design transfer optics for scalability. Figure 5 shows two equivalent fields of view with high scalability. In Fig. 5(a), three sub-SLMs are positioned in contact with each other diagonally and this unit SLM with three sub-SLMs is horizontally scalable since one unit SLM can be located closely to next other unit without the gap resulting from the lens pupil and the frame of SLM. Even though central directions of each local view are not included in the same plane, the asymmetric diffusing screen positioned at the focal plane removes the discrepancies in vertical direction and the consequent horizontal viewing angle is three times of the individual local view angle. In Fig. 5(b), though three sub-SLMs are piled up erectly, field of view is equivalent to that in Fig. 5(a). The mirrors being located in front of transfer lens reform an SLM effectively and this effectively reformed SLM has the same scalability as three sub-SLMs positioned in contact with each other diagonally. This novel design makes total viewing angle of stereogram be scalable by simply aligning effectively reformed SLMs on the curve in the same plane.

#96374 - $15.00 USD Received 19 May 2008; revised 26 Jul 2008; accepted 30 Jul 2008; published 1 Aug 2008

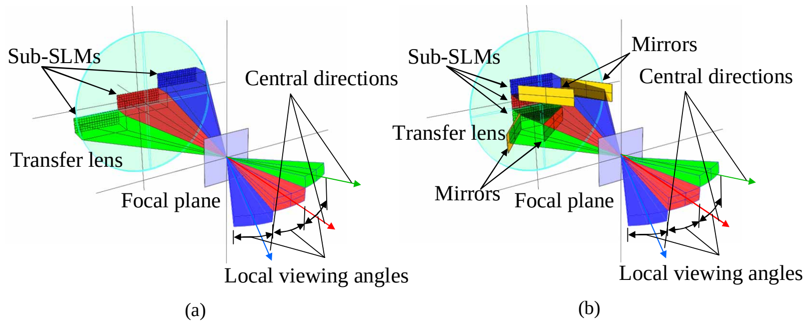

Fig. 5. Equivalent fields of view (a) by three sub-SLMs positioned at different vertical heights in contact with each other diagonally and (b) by effectively reformed SLM.

Figure 6 shows embodiment of effectively reformed SLM. In Fig. 6(a), the detailed structure is shown. This unit is composed of SLM, transfer lens, upper arm and lower arm. Both arms fold the transferred wave in front of the lens and the unit effectively reformed SLM generates three sub-views adjoining one another as shown in Fig. 6(b).

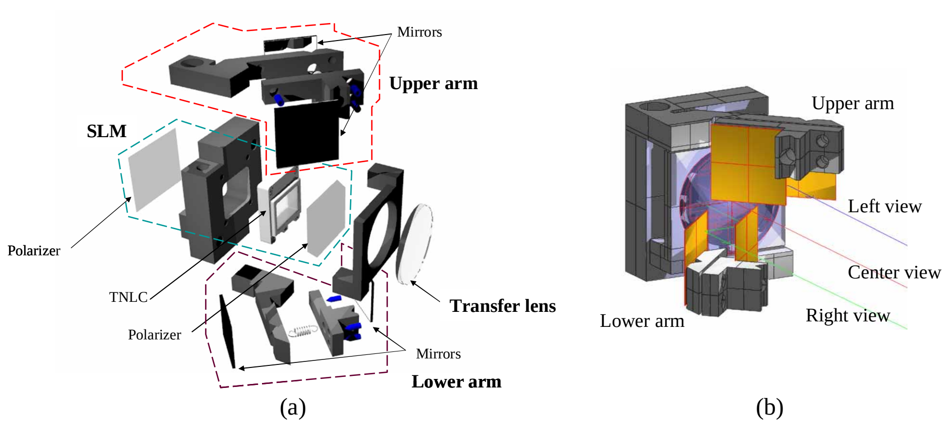

Fig. 6. Embodiment of effectively reformed SLM: (a) structure of effectively reformed SLM and (b) central directions of three sub-views.

Figure 7 shows central directions of local view in a curved array of effectively reformed SLM. Effectively reformed SLM has three central directions equivalent to three sub-SLMs positioned in contact with each other diagonally and their scalability is noticeable.

#96374 - $15.00 USD Received 19 May 2008; revised 26 Jul 2008; accepted 30 Jul 2008; published 1 Aug 2008

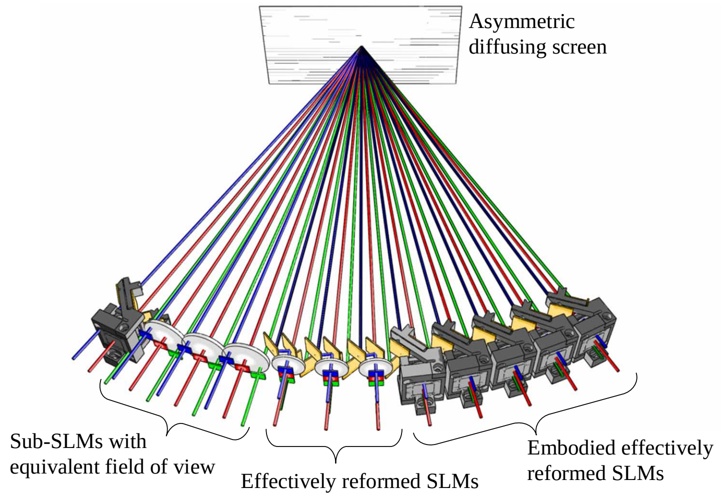

Fig. 7. Central directions of local view in a curved array of SLMs.

Figure 8 shows the quality deterioration in the upper arm of the effectively reformed SLM resulting from mirrors. The mirrors fold the modulated wave and tilt it with the angle of $\theta_U = 0.705^\circ$ from Eq. (9a). When the light waves pass through the mirrors, the gap between each mirror functions as an optical stop. This effective optical stop is located at $(l_1 + l_2 + l_3)$ distance away from the lens and its width w is equal to the width of SLM. The diffraction width from a single pixel of SLM at optical stop is given by

$$w' = \frac{\lambda}{p}\left[d + l_1 + l_2 + l_3 - \frac{d(l_1 + l_2 + l_3)}{f}\right]. \tag{20}$$

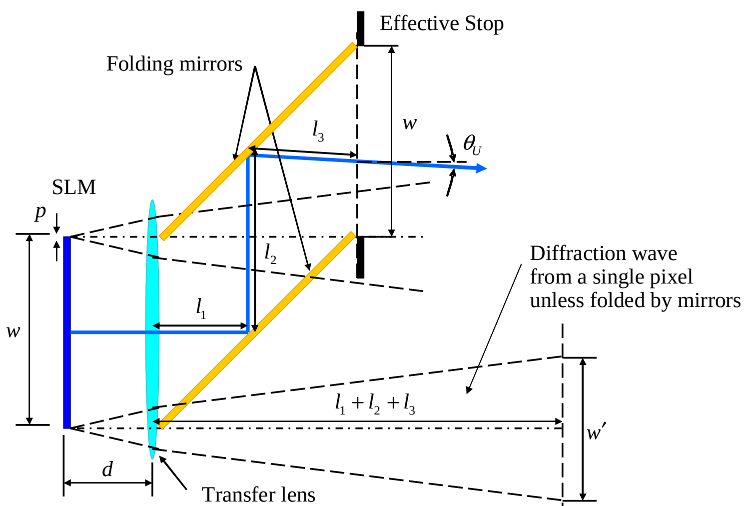

Fig. 8. Quality deterioration in upper arm of effectively reformed SLM resulting from mirrors.

In this paper, the width of SLM is $12.3mm$ and the diffraction width w' from a single pixel is $1.31mm$ from Eq. (20). Therefore, with the paraxial assumption that the information

#96374 - $15.00 USD Received 19 May 2008; revised 26 Jul 2008; accepted 30 Jul 2008; published 1 Aug 2008

of the diffraction wave from a single pixel is uniform over the full width w', the ratio of the whole information passing through the optical stop is formulated as

$$\int_{-w/2}^{w/2}\int_{-w/2}^{w/2} rect\left(\frac{x-u}{w'}\right)dxdu \Big/ \int_{-w/2}^{w/2}\int_{-\infty}^{\infty} rect\left(\frac{x-u}{w'}\right)dxdu = 1 - w'/4\,w. \tag{21}$$

Here, the ratio of the information displayed through the upper arm is about 97.4% and the quality deterioration caused by mirrors is about 2.6%. Therefore, the proposed effectively reformed SLM generates three views with the angle of 0.705° between each unit without significant quality deteriorations.

5. Embodiment of digital holographic display

In this section, the concept of the embodiment of digital holographic display with a curved array of effectively reformed SLM is explained. The characteristics of modulation in SLM are described and the display system with 4*f* optics for low loss division of the light source is presented.

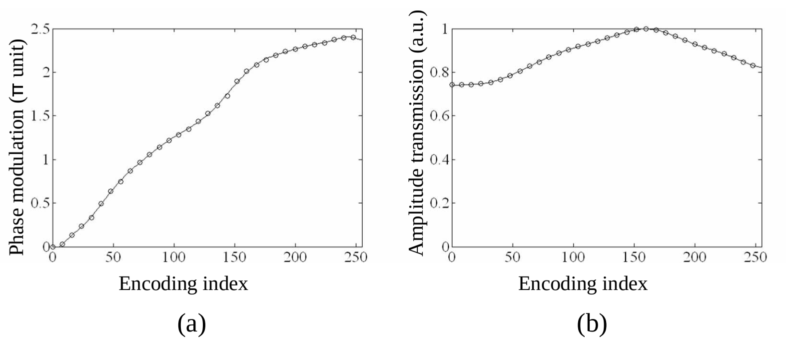

Fig. 9. Characteristics of SLM with (a) phase modulation and (b) amplitude transmission.

In this paper, Coherent DPSS Nd:YAG laser with the wavelength of $532nm$ is used as a light source, and the Epson L3P06X-55 is used as a twisted nematic liquid crystal (TNLC) in SLM, which has 1024×768 pixels with the pixel pitch of $12\mu m$. The rotation angles of input and output polarizers are 55 and 10 degrees for the SLM, respectively. The configuration of SLM is optimized with the genetic algorithm presented in Ref. 22. Figure 9 shows these resultant characteristics of SLM. The phase modulation covers the full range of 2π as shown in Fig. 9(a).

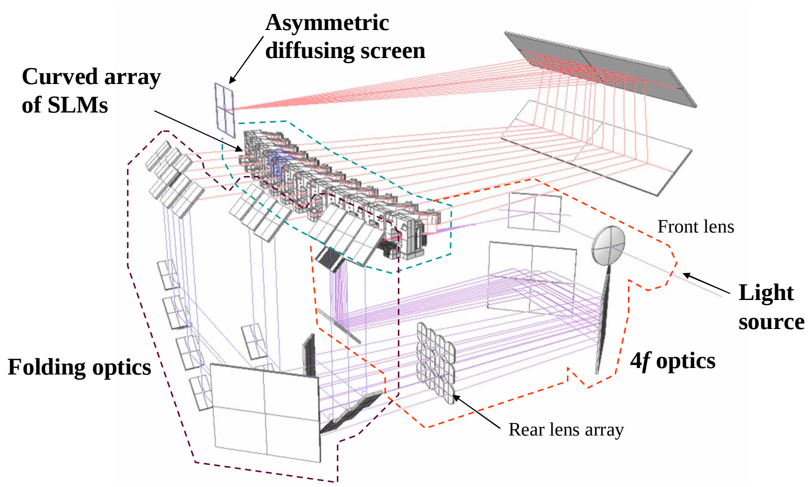

Fig. 10. Schematics of the proposed wide viewing angle dynamic holographic stereogram.

Figure 10 shows the schematics of the proposed wide viewing angle dynamic holographic stereogram. In this proposed system, the 4*f* optics is applied to divide the light source into every SLM. The 4*f* optics is composed of one front lens with focal length $250mm$ and twelve rear lenses in an array form with the focal length of $1000mm$. There is negligible loss of the light source to be divided into twelve collimated lights. In order to distribute these 2D arrayed beams to individual SLMs aligned on the curve with the radius of $1000mm$, folding optics is applied. As an asymmetric diffusing screen, holographic diffuser (Edmond Co.) is used. This screen diffuses the reconstructed wave vertically and provides an HPO display.

Figure 11 shows the pictures of the dynamic holographic stereogram. In Fig. 11(a), the array of effectively reformed SLMs is shown where units are mounted without upper arms for intelligibility. In Fig. 11(b), the whole system with electronic controllers is shown.

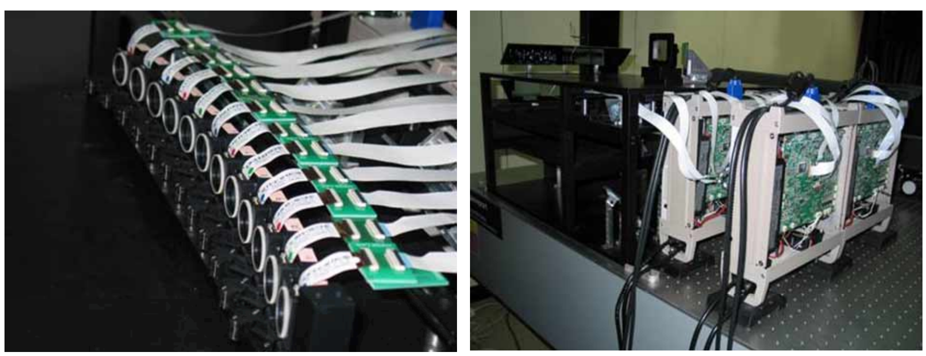

(a) (b)

Fig. 11. Pictures of the dynamic holographic stereogram: (a) the curved array of SLMs mounted without upper arms and (b) whole system with electronic controllers.

6. Experimental results

In this section, experimental results are presented. The configurations of triangle mesh-modeled 3D surface objects for generating digital hologram are described. Pictures and movie with the proposed digital holographic system are displayed.

#96374 - $15.00 USD Received 19 May 2008; revised 26 Jul 2008; accepted 30 Jul 2008; published 1 Aug 2008

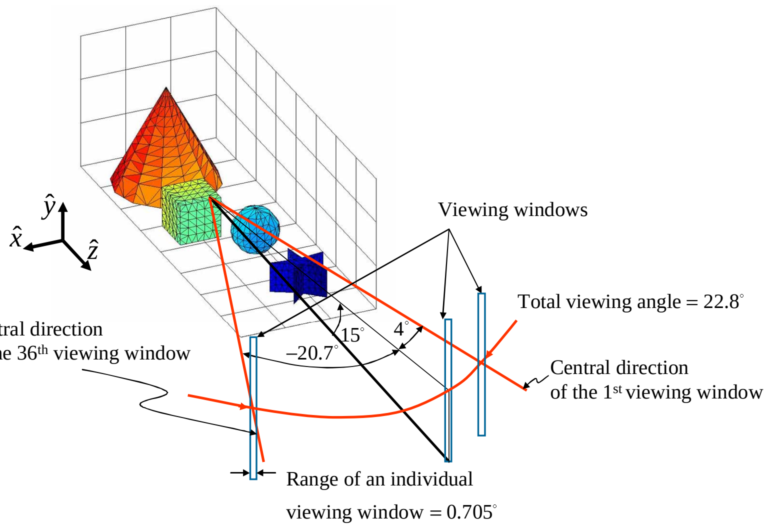

Fig. 12. Configuration of objects and definition of central directions to generate holograms.

In this paper, the technology to generate holograms from triangle mesh-modeled 3D surface objects is applied [23]. This technology is analogous to holographic stereograms from the viewpoints of restricting the angular spectrum of the object wave. This angular spectrum is equivalent to the object wave passing through a viewing window in holographic stereograms. Figure 12 shows the configuration of three-dimensional objects and the definition of central directions which are the central frequencies of angular spectrum in local view. In our proposed dynamic holographic stereogram with effectively reformed SLMs, every central direction is rotated at the regular interval of angle 0.705°, and there are 36 views generated by twelve SLMs. Therefore, the proposed dynamic holographic stereogram has wide viewing angle of 22.8° from Eq. (19).

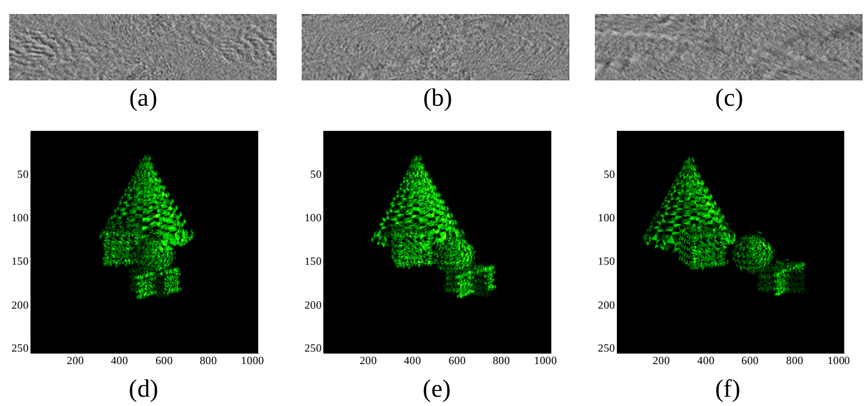

Fig. 13. Computer generated holograms and respective numerical reconstructions: holograms positioned at (a) the 1st, (b) the 19th, and (c) the 36th viewing directions. Parts (d) through (f) are correspondent images numerically reconstructed from parts (a) through (c), respectively.

Figure 13 shows the computer generated holograms and their numerically reconstructed images from the configurations in Fig. 12. These holograms are phase holograms with 8-bit level and have 1024×256 size which is one third of resolution in SLM. Figures 13(a) through (c) show holograms positioned at the 1st, 19th and 36th viewing directions respectively,

#96374 - $15.00 USD Received 19 May 2008; revised 26 Jul 2008; accepted 30 Jul 2008; published 1 Aug 2008

and Figs. 13(d) through 13(f) show numerically reconstructed images corresponding to Figs. 13(a) through 13(c).

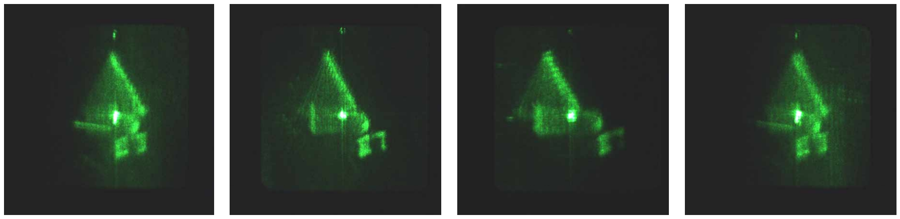

(a) (b) (c) (d)

Fig. 14. Pictures of the implemented dynamic holographic stereogram: (a) right view (b) center view and (c) left view. Part (d) is movie (1.83MB).

Figure 14 shows pictures and movie displayed on the proposed digital holographic display system. In our configuration, a filter is not used for obstructing the undiffracted wave, so the central peaks in Fig. 14 are undiffracted DC peaks. In Figs. 14(a) through (c), the pictures are in agreement with the numerically reconstructed images shown in Figs. 13(d) through (f). As expected, there is no discontinuity over the whole viewing angle of the proposed display.

7. Conclusion

With our proposed dynamic holographic stereogram, we achieve the wide continuous view, where the viewing angle is scalable simply by expanding the number of effectively reformed SLMs. The curved array of SLMs reduces the spatial bandwidth presented by a unit SLM and the wide angle view is displayed efficiently by local transforms with plural SLMs. This technique provides a feasible solution for the problem that it is hard to display a wide angle view with the conventional digital holography. The devised structure of effectively reformed SLMs makes the system scalable in viewing angle and compact. The loss of light power is significantly reduced when compared with previous researches. It is expected that the proposed technique can be useful in constituting a digital holographic display with wide viewing angle, and the scalability of optics can provide more degrees of freedom in designing the systems.

Acknowledgment

This work was supported by Samsung SDI, Ltd. and Brain Korea 21 Program (Information Technology) of the Korean Ministry of Education, Science and Technology.

#96374 - $15.00 USD Received 19 May 2008; revised 26 Jul 2008; accepted 30 Jul 2008; published 1 Aug 2008